1 of 1

KAPL-4762
UC-901, Chemistry
(DOE/OSTI-4500-R75)

Zinc(II) Oxide Stability in Alkaline Sodium Phosphate Solutions at Elevated Temperatures

S. E. Ziemniak
E. P. Opalka

April 1993

Prepared for
The United States Department of Energy

Prepared by
Knolls Atomic Power Laboratory
P. O. Box 1072
Schenectady, New York

Contract No. DE-AC12-76-SN00052

DISCLAIMER

CONTENTS

ILLUSTRATIONS

TABLES

ABSTRACT

Zinc oxide (ZnO) is shown to transform into either of two phosphate-containing compounds in relatively dilute alkaline sodium phosphate solutions at elevated temperatures via

$$ZnO(s) + Na^+ + H_2PO_4^- \rightleftarrows NaZnPO_4(s) + H_2O$$

or

$$2\ ZnO(s) + H_3PO_4(aq) \rightleftarrows Zn_2(OH)PO_4(s) + H_2O.$$

X-ray diffraction analyses indicate that $NaZnPO_4$ possesses an orthorhombic unit cell having lattice parameters a = 8.710 $\pm$0.013, b = 15.175 $\pm$0.010, and c = 8.027 $\pm$0.004 Å.

The thermodynamic equilibria for these reactions were defined in the system ZnO-Na_2O-P_2O_5-H_2O for Na/P molar ratios between 2.1 and 3. Based on observed reaction threshold values for sodium phosphate concentration and temperature, the standard entropy (S°) and free energy of formation (ΔG_f°) for $NaZnPO_4$ were calculated to be 169.0 J/mol-K and -1510.6 kJ/mol, respectively; similar values for $Zn_2(OH)PO_4$ (tarbuttite) were 235.9 J/mol-K and -1604.6 kJ/mol. Additions of sodium sulfite and sulfate did not alter the above reactions.

KEY WORDS: zinc(II) oxide, zincite, sodium zinc phosphate, tarbuttite, aqueous solutions, sodium orthophosphate, thermodynamics, equilibrium constant, corrosion, hydrothermal solutions.

ACKNOWLEDGEMENT

We are indebted to the following individuals who contributed professional assistance: P. C. Sander for X-ray diffraction analyses; Dr. J. J. Cheung for infrared spectroscopy; G. M. Neugebauer for scanning electron microscopy; and V. P. Nordstrom for electron microprobe quantitative chemical analyses.

ZINC(II) OXIDE STABILITY IN ALKALINE SODIUM PHOSPHATE SOLUTIONS AT ELEVATED TEMPERATURES

INTRODUCTION

Recent investigation of the solubility/phase behavior of zinc(II) oxide in alkaline sodium phosphate solutions[1] established a $ZnO/NaZnPO_4$ phase boundary in terms of an equilibrium constant for the liquid phase composition: $[Na^+][H_2PO_4^-]$. According to Thilo and Schulz[2], precipitation of a second basic salt of zinc(II) oxide, $Zn_2(OH)PO_4$ (tarbuttite), is possible under mildly-alkaline, hydrothermal conditions. A hydrous form of this mineral is also known to exist: $Zn_2(OH)PO_4 \cdot 1.5\ H_2O$ (spencerite).

The present work was undertaken to determine: (a) the manner in which sulfur oxyanion salts (sulfate and sulfite) affect formation of $NaZnPO_4$, and (b) whether a sodium-free zinc phosphate compound would form in the system $ZnO\text{-}Na_2O\text{-}P_2O_5\text{-}H_2O$ for $2 < Na/P < 3$.

EXPERIMENTAL

Autoclave Tests

All tests were conducted in a one-liter, gold-lined autoclave vessel fitted with a platinum 'dip' tube to permit hot sampling. A sketch of the apparatus is shown in Figure 1. The experimental methodology was the same as that described previously[3], viz., incrementally elevate the temperature of a sodium phosphate solution in contact with a ZnO powder reactant until a phosphate loss is observed.

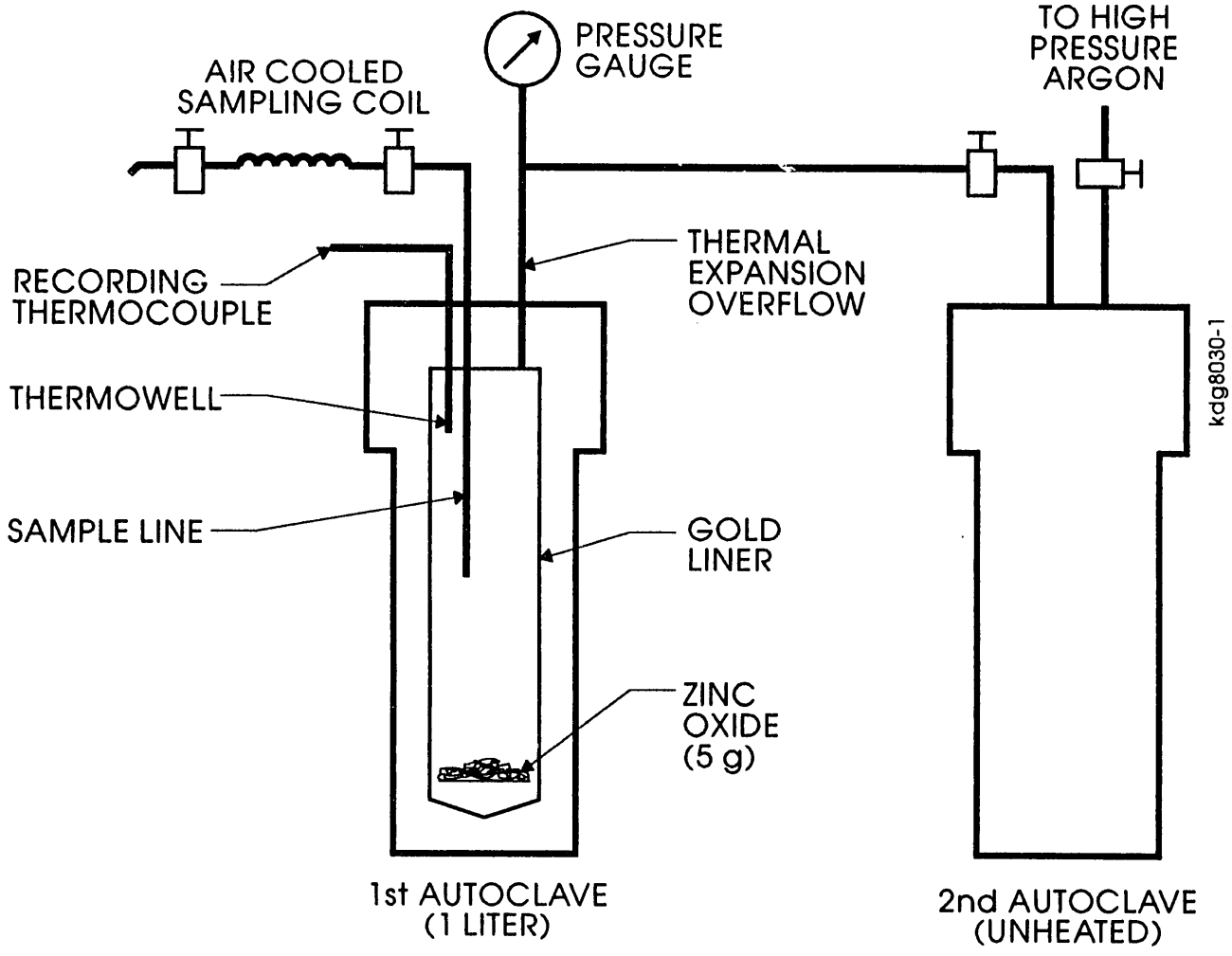

FIGURE 1 Schematic of Autoclave Arrangement Used in Zinc Oxide Transformation Study

Reagents

Demineralized and deaerated water (resistivity > 1 Mohm-cm) was used to prepare all test solutions used in our experiments. All chemicals used [ZnO, Na_2HPO_4 (anhyd.), $Na_3PO_4 \cdot 12H_2O$, Na_2SO_3, and Na_2SO_4 (anhyd.)] were of analytical or equivalent grade obtained from Fisher Scientific Company or the GSA Chemical Commodities Agency. Zinc oxide was tested in its as-received condition.

Analytical Procedures

The total phosphate concentration and sodium-to-phosphate molar ratio (Na/P) of each sample aliquot were determined by the potentiometric-titration procedure described previously[3]. The existence of lower phosphate concentrations, however, made it prudent to titrate larger aliquots (up to 50 gms solution) in order to achieve the stated accuracies.

The above procedure was modified for sulfite determination (in the presence of phosphate), based on the reaction with formaldehyde:

$$SO_3^{2-} + CH_2O + H_2O \rightleftarrows (CH_2OH)(SO_3^-) + OH^- \quad (1)$$

After titrating to the first phosphate hydrolysis point at pH = 9.2 $\pm$0.1, sufficient formaldehyde was added to the liquid sample to react completely with the sulfite. The hydroxyl ions thus liberated, increased the solution pH which was then titrated back to the original pH = 9.2 $\pm$0.1 value. The equivalent amount of titrant used was equal to the amount of sulfite present. The expected accuracy of this procedure is $\pm$3%. Sulfate ion concentrations were determined by ion chromatographic analysis with an accuracy of $\pm$10%.

Upon completion of each autoclave experiment, the reacted zinc oxide powder was rinsed with deionized water to remove any traces of unreacted sodium phosphate and subjected to

visual examination under a stereomicroscope. A portion of the reaction 'cake' was then fractured and isolated for characterization by X-ray diffraction (XRD) analysis. Powder XRD measurements were performed using a Model CN2155D5 Rigaku diffractometer (Bragg-Brentano geometry) and Cu Kα radiation (λ = 1.5417 Å). The X-ray tube was operated at 45 kV and 20 ma. Data were taken as a continuous scan from 8 to 92 deg (2θ) at a speed of 1 deg/minute.

In an attempt to react to completion, Test 4 was charged with 2 gms of ZnO, rather than 5 gms, and operated for a total of 7 days. The reaction product from this test was subjected to additional characterizations by infrared spectroscopy (ir) and quantitative chemical analyses. The solids ir spectrum was obtained on a Perkin-Elmer Model 283 spectrometer using the KBr pellet technique. Elemental chemical microanalyses were performed by Galbraith Laboratories, Inc. (Knoxville, TN).

RESULTS

Zinc Oxide Phase Boundary I

Threshold temperatures at which sodium phosphate precipitation was initiated, were determined by reverse extrapolation of phosphate concentration versus temperature plots. At least three temperature points above the threshold levels were included from each run. This process is illustrated in Figure 2. Based on changes in the Na/P ratios of the depleted test solutions, compared with initial (baseline) values, indicated Na/P loss ratios were calculated. These values, along with the estimated ZnO transformation temperatures, are summarized in Table I. No losses of any sulfur oxyanion species (sulfate or sulfite) were observed.

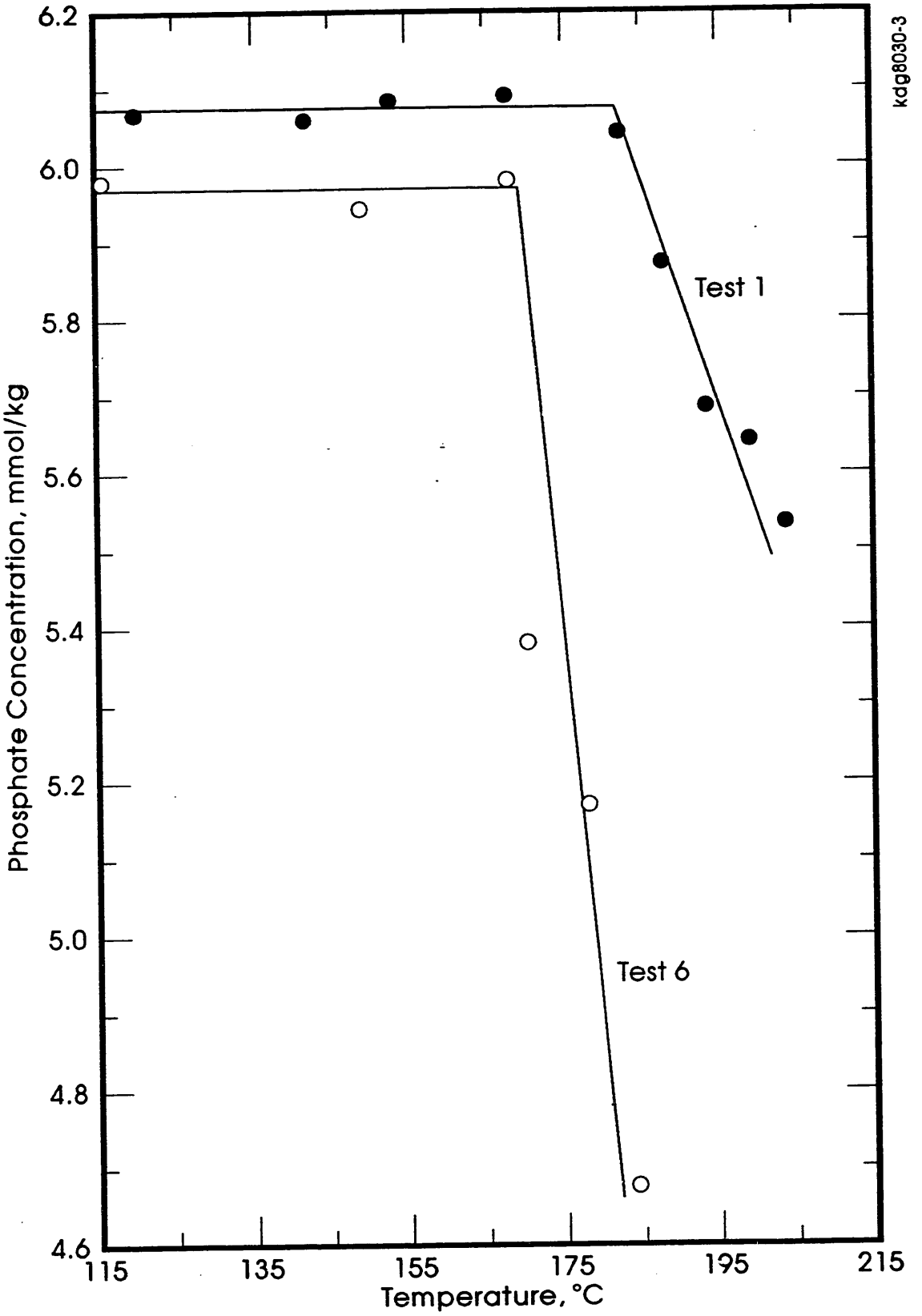

FIGURE 2. Phosphate Variations Caused by Heating in the Presence of Zinc(II) Oxide

TABLE I. Zinc(II) Oxide Phase Transformation Thresholds

Test	Baseline Phosphate*	Na/P	Threshold Temp. K.	Final Phosphate*	Na/P	Indicated Na/P Loss
1	6.076	2.159	455	3.928	2.775	1.0
2	6.507	2.513	482	3.980	3.748	0.6
3	6.339	2.781	472	3.433	4.260	1.0
4	111.6	2.166	353	85.29	2.540	1.0
5	6.223	2.158 (1)	400	4.349	2.623	1.1
6	5.970	2.458 (2)	443	4.675	2.887	0.9
7	6.781	2.202 (3)	439	5.212	3.300	(5)
8	5.517	2.452 (4)	455	3.780	3.153	0.9

* mmol/kg; Na/P ratio excludes sodium contributed by sulfur oxyanion salts: (1) sulfate = 6.933, (2) sulfate = 7.110, (3) sulfite = 8.593, (4) sulfite = 5.333; (5) Na/P loss calculation invalid due to suspected leaching of sodium phosphate from system crevices from a previous run that used extremely high phosphate concentrations.

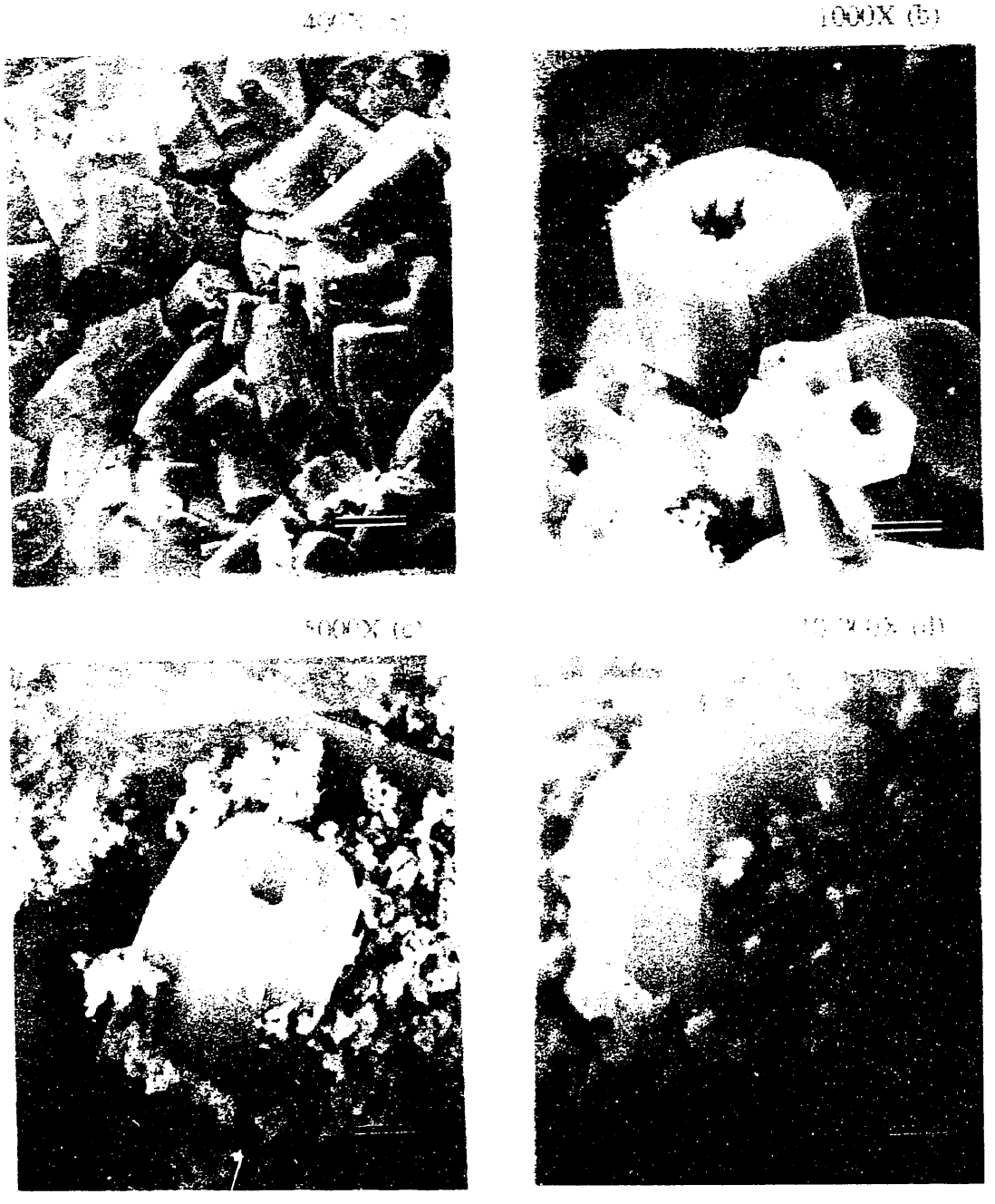

FIGURE 3 Scanning Electron Micrographs of Zinc Oxide-Sodium Phosphate Reaction Products. Bar length corresponds to 25 μm, 10 μm, 2 μm and 1μm in Figs. (a) - (d), respectively.

The above results indicate that the zinc oxide-sodium phosphate reaction product from all 8 tests contained sodium and phosphate in a 1:1 molar ratio. Test 4, which decomposed the entire 0.025 mole charge of ZnO, precipitated approximately 0.026 mole of phosphate from solution. This result indicates a reaction product composition Zn/P $\approx$ 1.

Characterization of Reaction Product I

Individual microcrystals of the reaction product, when viewed under a stereomicroscope, appeared white and translucent. SEM photographs of representative reaction product crystals are provided in Figure 3 at magnifications between 400 and 10,000X. These photographs reveal the crystals to have a barrel-like appearance. In most instances the 'barrels' have a hexagonal cross-section, a hollow center, and an l/d ratio of approximately 2/1. Crystal sizes (5 - 25 μm diam.) are relatively large in comparison to the unreacted zinc oxide (0.5 μm); see Figure 3d.

XRD analyses, as performed with monochromatic copper K_α X-rays, revealed that the zinc oxide decomposition products from Tests 1-8 had identical crystalline lattice configurations; that is, they were the same compound. Only in Test 4 were the peak intensities sufficiently strong to provide an X-ray diffraction pattern useful for reference purposes; see Table II. A search of the JCPDS database[4] revealed that, although the reaction product possessed some similarities with the α-$NaZnPO_4$ compound generated by Kolsi et al[5] under non-hydrothermal conditions, the interplanar spacings are most consistent with the $Na(Zn_{0.8}Fe_{0.2})PO_4$ compound generated by Kabalov et al[6] via a hydrothermal synthesis. Their reported crystal symmetry is monoclinic with unit cell lattice parameters of a = 8.668

TABLE II

Indexed Powder X-Ray Diffraction Pattern of
Zinc(II) Oxide-Sodium Phosphate Reaction Product

Measured Pattern		Reflection Plane Indices			Calculated
d-Spacing Å	Rel. Intens. I/I_o	h	k	l	d-Spacing Å
5.88	6	1	0	1	5.903
4.646	35	1	2	1	4.659
4.360	65	2	0	0	4.355
		1	3	1	4.374
4.008	80	0	0	2	4.014
3.883	17	0	1	2	3.880
3.710	18	2	1	1	3.712
3.290	11	1	2	2	3.286
3.198	14	1	4	1	3.192
3.147	6	0	3	2	3.144
3.058	6	2	3	1	3.052
2.959	100	2	0	2	2.952
		1	3	2	2.958
2.863	18	2	4	0	2.860
		1	5	0	2.866
2.629	20	1	4	2	2.629
2.522	70	1	1	3	2.522
		0	2	3	2.524
2.414	31	0	6	1	2.413
2.331	7	2	4	2	2.330
		1	5	2	2.332
2.280	8	2	0	3	2.280
		1	3	3	2.283

TABLE II (Continued)

Measured Pattern d-Spacing Å	Rel. Intens. I/I_o	Reflection Plane Indices h	k	l	Calculated d-Spacing Å
2.252	20	2	1	3	2.255
2.182	9	2	2	3	2.184
2.117	27	2	5	2	2.116
2.007	6	0	0	4	2.007
		0	5	3	2.007
1.989	10	0	1	4	1.990
1.922	14	2	6	2	1.920
1.834	5	3	3	3	1.834
1.824	9	2	0	4	1.823
		1	3	4	1.824
		2	5	3	1.823
1.676	14	0	5	4	1.674
1.650	5	3	0	4	1.651
		4	2	3	1.649
		3	5	3	1.651
		4	6	0	1.650
		0	9	1	1.650
1.573	6	1	1	5	1.570
		0	2	5	1.571
		0	6	4	1.572
		2	9	0	1.572
1.528	14	1	9	2	1.530
1.508	23	2	0	5	1.506
		1	3	5	1.507
		4	7	1	1.509
1.460	16	5	0	3	1.460
		1	4	5	1.458

± 0.006, b = 8.125 ± 0.004, and c = 15.281 ± 0.001 Å; ß = 90.17 deg. An indexing of the Table II X-ray diffraction pattern by means of the DICVOL computer code[7] obtained a satisfactory fit with an orthorhombic unit cell having lattice parameters a = 8.710 ± 0.013, b = 15.175 ± 0.010, and c = 8.027 ± 0.004 Å (i.e., ß = 90 deg). The figure of merit for this fit (F_{31} = 4.6) is consistent with an average (absolute) discrepancy in 2θ of 0.028 deg.

Standard quantitative chemical analyses of the Test 4 reaction product performed after digestion in nitric acid yielded:

Element	wgt %	Atom Ratio to P
Na	11.10	0.94
P (as PO_4)	15.88 (49.50)	-
Zn	37.19	1.11
	Total 97.8	

A Zn/P atom ratio slightly in excess of unity, along with approximately 2% unaccounted for material (assumed to be oxygen), is consistent with the presence of 5-10% unreacted ZnO in the Test 4 reaction cake. The absence of hydroxyl ions was inferred from the absence of an infrared absorption peak in the vicinity of 3500 ± 100 cm^{-1}, which corresponds to the expected stretching frequency of the O-H bond. This result is also consistent with the quantitative elemental results.

Assembly of the above information gives the ZnO decomposition product stoichiometry as Na/P = Zn/P = 1, or $NaZnPO_4$.

Zinc Oxide Phase Boundary II

Three additional tests were conducted using lower phosphate concentrations; see Table III. As expected, lower phosphate concentrations led to higher reaction threshold temperatures. However, the inferred reaction product composition differed from the preceding results in that no sodium losses were observed. The reaction appeared to be self-limiting, undoubtedly due to the relatively large increases in solution Na/P ratios created by the reaction. That is, the higher Na/P ratios created a test environment where the ZnO phase was once again stable.

Characterization of Reaction Product II

The extremely small amounts of phosphate reacted in this three run series (avg = 0.3 mmole P) made a positive identification by bulk analysis very difficult. XRD analyses of selected regions of the ZnO 'cakes' enriched with reaction products, however, confirmed that the reaction product's major lines were coincident with the major (i.e., $I/I_0 > 10\%$) lines of synthetic tarbuttite[8]; see Table IV.

Chemical analyses of individual microcrystals of the reaction product were performed using a JEOL Model JXA-8600 Electron Microprobe operated at 15 kV. The results indicated the following atomic ratios: Zn/P = 2.2, O/P = 4.5, with estimated uncertainties of $\pm 15\%$ (1σ). Only trace levels of sodium were detected, i.e., <5%. Therefore, the above analyses confirm that the second ZnO decomposition product is tarbuttite, $Zn_2(OH)PO_4$.

TABLE III. Additional Zinc(II) Oxide Reaction Thresholds

Test	Baseline Phosphate	Baseline Na/P	Threshold Temp., K	Final Phosphate	Final Na/P	Indicated Na/P Loss
9	2.864	2.164	494	2.611	2.538	-1.7
10	2.611	2.453	528	2.316	2.750	0.1
11	1.885	2.150	481	1.485	2.735	0.0

TABLE IV. Comparison of Powder X-Ray Diffraction Patterns of Second Zinc(II) Oxide-Sodium Phosphate Reaction Product and Synthetic Tarbuttite

Synthetic Tarbuttite[8]		Composite Pattern of Tests 9-11	
d-Spacing Å	Rel. Intensity I/I_o	d-Spacing Å	Rel. Intensity I/I_o
6.18	100	6.14	35
5.37	15	5.42	25
4.59	12	4.58	20
3.69	45	3.68	85
3.266	70	3.26	90
2.971	40	2.97	35
2.876	45	*	*
2.771	40	*	*
2.928	15	*	*
2.471	50	*	*
2.416	30	2.43	20
2.355	15	2.354	40
2.055	30	2.054	25

*Obscurred by overlap with ZnO line.

DISCUSSION

The present experiments demonstrate that zinc(II) oxide was decomposed by relatively dilute sodium phosphate solutions. Based on observed reaction product stoichiometries, two ZnO decomposition reaction equilibria were isolated:

$$ZnO(s) + Na^+ + H_2PO_4^- \rightleftharpoons NaZnPO_4(s) + H_2O \quad (2)$$

or

$$2ZnO(s) + H_3PO_4(aq) \rightleftharpoons Zn_2(OH)PO_4(s) + H_2O \quad (3)$$

The existence of other ZnO decomposition products, such as $NaZn_2(PO_4)(HPO_4)$ and $Na_2Zn(OH)PO_4$, which have been hydrothermally synthesized in the respective phosphoric acid[9] and trisodium phosphate[10] solutions, has been ruled out because of their nonrepresentative Na/P ratios.

Equilibrium constants for Eqns. (2) and (3) were defined by:

$$K_{(2)} = \frac{a_{NaZnPO_4} a_{H_2O}}{a_{ZnO} a_{Na^+} a_{H_2PO_4^-}} \quad (4)$$

and

$$K_{(3)} = \frac{a_{Zn_2(OH)PO_4} a_{H_2O}}{a^2_{ZnO} a_{H_3PO_4}} \quad (5)$$

In the usual manner, activities (a_i) of water and all solid phases were taken to be unity, whereas ionic activity coefficients (γ_i) were used to relate ionic concentrations [C_i] to thermodynamic activities. Marshall and Jones[11] have shown that an extended Debye-Huckel

equation of the form:

$$\log \gamma_i = -Z_i^2 S \sqrt{I} \,/\, (1 + A\sqrt{I}) \tag{6}$$

with A = 1.5 gives reasonable approximations at temperatures in the range 400 - 500 K for ionic strengths ($I = 0.5\ \Sigma\ C_i Z_i^2$) typical of our tests. In Eqn. (6), Z_i is the ionic charge number and S is the limiting Debye-Huckel slope (0.51 at 298 K)[12].

Combining Eqns. (2) - (6) yields:

$$\log K_{(2)} = \log Q_{(2)} + 2S\sqrt{I} \,/\, (1 + 1.5\sqrt{I}) \tag{7}$$

where

$$\log Q_{(2)} = -\log [Na^+]\,[H_2PO_4^-]$$

and

$$\log K_{(3)} = -\log [H_3PO_4] \tag{8}$$

An ion electroneutrality balance, which accounted for changes in water[12], phosphate ion[13,14], and sulfur oxyanion[15,16] dissociation behavior with temperature and ionic strength, was then employed to determine $H_2PO_4^-$ and H_3PO_4(aq) concentrations at the Tables I and III threshold conditions. For the most general case, with sodium phosphate and sodium sulfite present, the balance is

$$[H^+] + [Na^+] = 3[PO_4^{3-}] + 2[HPO_4^{=}] + [H_2PO_4^-] + 2[SO_3^{=}] + [HSO_3^-] + [OH^-] \tag{9}$$

This balance was converted to a mathematical equation by introducing the following equilibrium constants:

$$K_w = (H^+)(OH^-) \qquad K_1 = \frac{(H_2PO_4^-)}{(H_3PO_4(aq))(OH^-)}$$

$$K_I = \frac{(H^+)(HSO_3^-)}{(H_2SO_3(aq))} \qquad K_2 = \frac{(HPO_4^=)}{(H_2PO_4^-)(OH^-)} \tag{10}$$

$$K_{II} = \frac{(H^+)(SO_3^=)}{(HSO_3^-)} \qquad K_3 = \frac{(PO_4^{3-})}{(HPO_4^=)(OH^-)}$$

with $\log K_i = b_1/T + b_2 + b_3 \ln T + b_4 T + b_5/T^2$.

The above parameters are tabulated in Table V. Upon substitution of the Eqn. (10) dissociation constants into Eqn. (9) and applying the known levels of total dissolved sulfite (m_s) and phosphate (m_p) (and its associated sodium-to-phosphate molar ratio, y), the neutrality balance reduced to an algebraic equation in terms of the unknown $[H^+]$, i.e., x:

$$x + (y-3)m_p = \frac{-m_p\left[1+\left(2-\frac{3x}{K_wK_1}\right)\frac{x}{K_wK_2}\right]\frac{x}{K_wK_3}}{1+\left[1+\left(1+\frac{x}{K_wK_1}\right)\frac{x}{K_wK_2}\right]\frac{x}{K_wK_3}} \qquad \frac{-m_s\left(1+\frac{2x}{K_I}\right)\frac{x}{K_{II}}}{1+\left(1+\frac{x}{K_I}\right)\frac{x}{K_{II}}} + \frac{K_w}{x} \tag{11}$$

Eqn. (11) represents a seventh order polynomial equation in terms of the unknown, x, and was solved by a Newton-Raphson iteration procedure. The calculated reaction threshold values for $[H^+]$, along with those for $[H_2PO_4^-]$ and $[H_3PO_4(aq)]$, are given in Table VI. It is noted that measured and calculated pH values (at room temperature) for all baseline test solutions agreed to within the reproducibility of the measurements (± 0.05). All ΔG values reported in the final column of Table VI were determined from the expression

TABLE V. Dissociation Behavior of Selected Compounds

K_i	b_1	b_2	b_3	b_4	b_5	Reference Cited
K_w	31,286.0	-606.522	94.9734	-0.097611	-2,170,870	Sweeton, Mesmer and Baes[12]
K_1	17,655.8	-253.198	39.4277	-0.0325405	-810,134	Mesmer and Baes[13]
K_2	17,156.9	-246.045	37.7345	-0.0322082	-897,579	Mesmer and Baes[13]
K_3	-106.51	7.1340	-	-0.017459	-	Treloar[14]
K_I	-1424.4	10.192	-	-0.024982	-	Khodakovskii, Ryzhenko and Naumov[15]
K_{II}	-1629.1	5.733	-	-0.025214	-	Khodakovskii, Ryzhenko and Naumov[15]
K_I (sulfate)	593,089	-8850.82	1343.462	-1.019062	-43,593,400	Izatt, Christensen, Oscarson, and Gillespie[16]
K_{II} (sulfate)	119,452	-1974.81	305.682	-0.275677	-7,715,600	Izatt, Christensen, Oscarson, and Gillespie[16]

TABLE VI

Solution Chemistry Values Used to Define the
$ZnO/NaZnPO_4$ and $ZnO/Zn_2(OH)PO_4$ Phase Boundaries

Test	$[Na^+]$ m	$[H_2PO_4^-]$ m	log Q_1	I	S	ΔG, kJ/mol
1	1.312×10^{-2}	5.815×10^{-4}	5.1173	0.01861	0.7640	-46.08
2	1.635×10^{-2}	5.128×10^{-4}	5.0767	0.02243	0.8374	-48.73
3	1.763×10^{-2}	2.851×10^{-4}	5.2992	0.02369	0.8057	-49.60
4	2.418×10^{-1}	2.188×10^{-5}	5.2765	0.3711	0.5798	-38.71
5	2.730×10^{-2}	1.258×10^{-4}	5.4642	0.04034	0.6424	-43.03
6	2.889×10^{-2}	2.179×10^{-4}	5.2010	0.04177	0.7355	-46.06
7	3.212×10^{-2}	1.124×10^{-4}	5.4424	0.04314	0.7265	-47.67
8	2.419×10^{-2}	1.391×10^{-4}	5.4730	0.03123	0.7640	-49.53
			$[H_3PO_4]$			
9	6.198×10^{-3}	8.260×10^{-4}	8.795×10^{-9}	0.00824	-	-76.18
10	6.405×10^{-3}	9.204×10^{-4}	1.320×10^{-8}	0.00810	-	-79.64
11	4.053×10^{-3}	5.868×10^{-4}	7.052×10^{-9}	0.00535	-	-75.06

$$\Delta G_i = -RT\ln K_i \qquad (12)$$

Least-squares fits of the Table VI results (see Figures 4 and 5) yield:

$$ZnO/NaZnPO_4: \quad \Delta G(kJ/mol) = -8522 \pm 5395 - (86.06 \pm 12.28)T \qquad (13)$$

$$ZnO/Zn_2(OH)PO_4: \quad \Delta G(kJ/mol) = -27640 \pm 1698 - (98.44 \pm 3.39)T \qquad (14)$$

Eqn. (13) provides free energy changes for Eqn. (2) with an estimated standard deviation of ± 1.15 kJ/mol over the temperature range 350 - 490 K. An independent estimate of the Eqn. (2) equilibrium, based on our previous ZnO solubility study[1], is plotted for comparison purposes in Figure 4. Given the precision of the latter estimate ($1\sigma = \pm 3.0$ kJ/mol), the observed 2 kJ/mol difference between the two correlations is not significant. Combination of the above results with previously established thermodynamic properties yields the summary presented in Table VII.

The observed susceptibility of ZnO to hydrothermal degradation in alkaline sodium phosphate solutions has led to the precipitation of sodium-zinc(II)-phosphate phases that are unique with respect to neighboring divalent transition metal ions: Na^+ and OH^- have not precipitated concurrently. That is, $Na_2Zn(OH)PO_4$ was not observed. Although the latter compound has been hydrothermally formed in trisodium phosphate and sodium sulfate solutions[10], the present results confirm that $NaZnPO_4$ is the preferred zinc(II) oxide decomposition product at lower solution alkalinities.

It is noteworthy that the orthorhombic structure of $NaZnPO_4$ is virtually identical to that possessed by beryllonite ($NaBePO_4$)[25]: a = 8.16, b = 14.08, and c = 7.79 Å; the lower

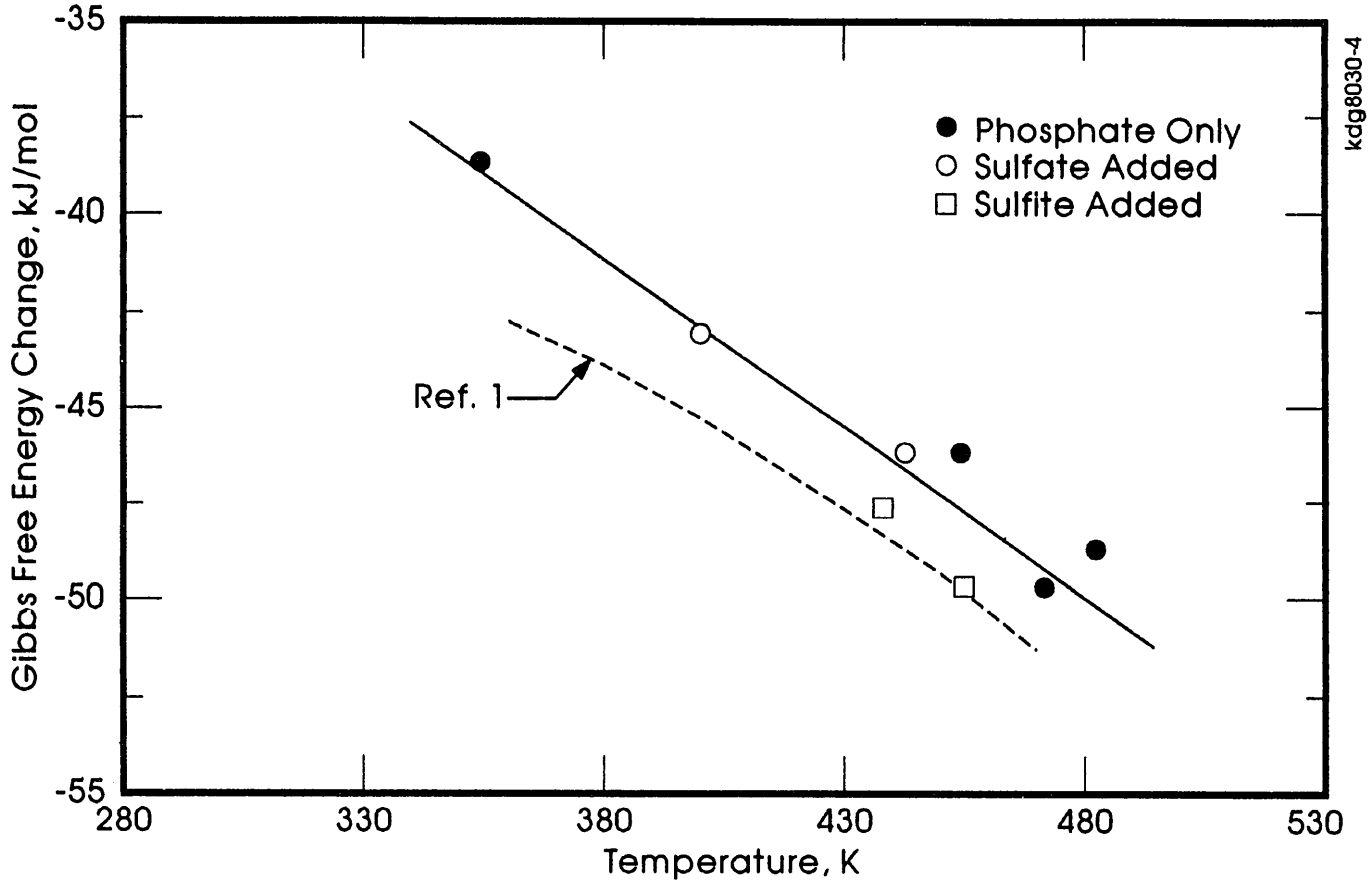

FIGURE 4. Free Energy Changes Determined for Zincite Transformation to Sodium-Zinc-Phosphate in Alkaline Sodium Phosphate Solutions

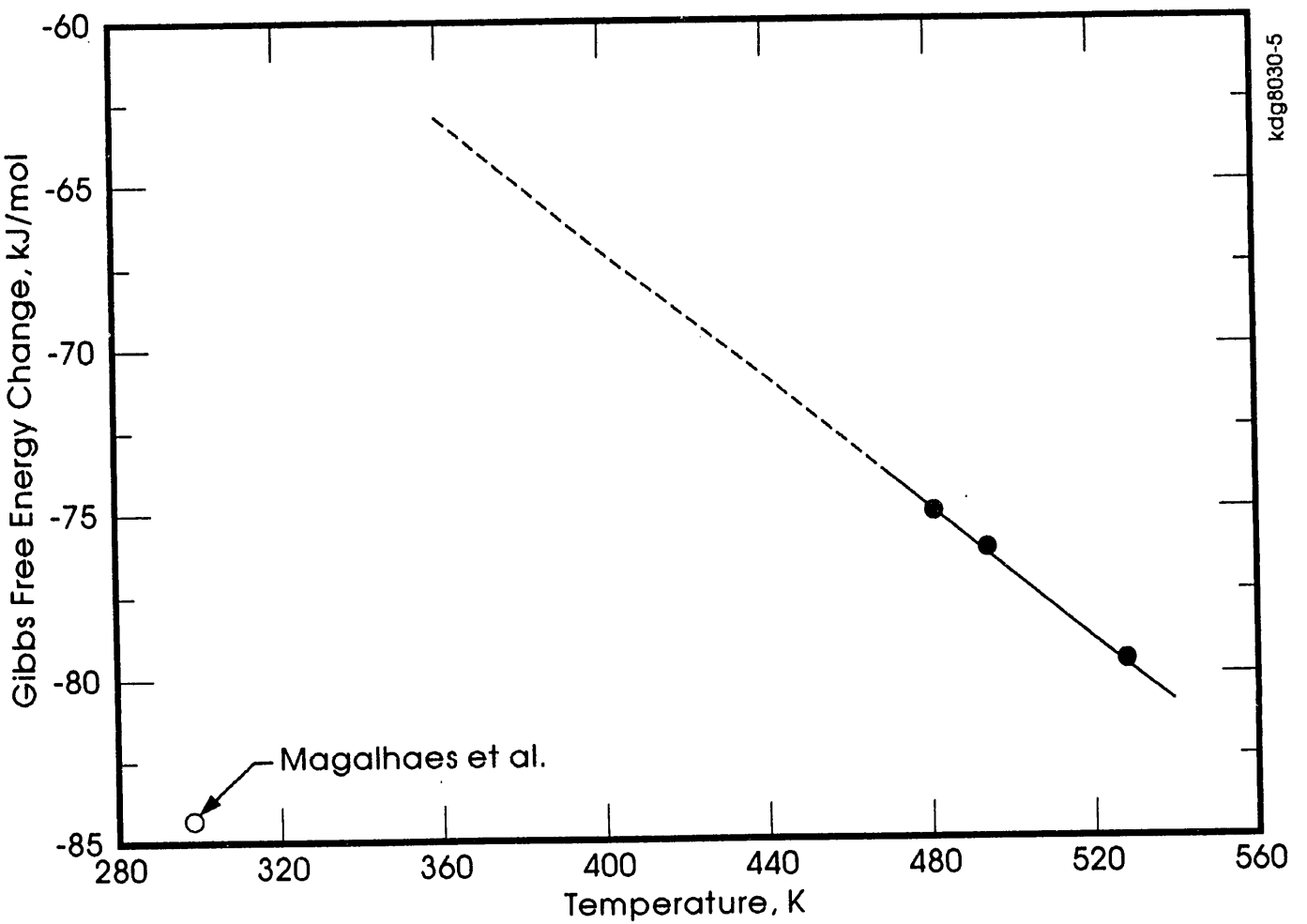

FIGURE 5. Free Energy Changes Determined for Zincite Transformation to Dizinc Hydroxyphosphate (Tarbuttite) in Alkaline Sodium Phosphate Solutions

TABLE VII. Thermochemical Parameters for Selected Species in the $ZnO-Na_2O-P_2O_5-H_2O$ System

Species	$C_p°(298)$ $J\text{-}mol^{-1}\text{-}K^{-1}$	$S°(298)$ $J\text{-}mol^{-1}\text{-}K^{-1}$	$\Delta H_f°(298)$ $kJ\text{-}mol^{-1}$	$\Delta G_f°(298)$ $kJ\text{-}mol^{-1}$	Reference Cited
$H^+(aq)$	-71 ± 1	-22.2	0	0	17,18
$Na^+(aq)$	-24.6	36.8	-240.12	-261.91	19
$Zn^{2+}(aq)$	-164	-154.8 ± 1.3	-153.64 ± 0.42	-147.23	18,20
$H_2(g)$	28.83	130.58 ± 0.08	0	0	21
$O_2(g)$	29.37	205.02 ± 0.4	0	0	21
H_2O	75.31	69.96 ± 0.08	-285.85 ± 0.04	-237.19 ± 0.04	21
$PO_4^{3-}(aq)$	-283 ± 20	-153.6	-1277.4	-1018.8	19,22
$HPO_4^{2-}(aq)$	-112 ± 4	-32.6	-1305.5	-1089.7	14,22
$H_2PO_4^-(aq)$	37 ± 4	72.4	-1308.8	-1130.8	13,22
$H_3PO_4(aq)$	94 ± 4	119.8	-1300.2	-1143.0	13,22
Na(s)	28.24	51.21	0	0	19
P(s)	23.84	41.09	0	0	19
Zn(s)	23.40	41.63 ± 0.21	0	0	21
$\xi\text{-}Zn(OH)_2(s)$	72.4	76.99 ± 0.21	-645.47	-555.93 ± 0.21	20
ZnO(s)	40.25	43.64 ± 0.42	-350.83 ± 0.21	-320.91 ± 0.25	21
$\alpha\text{-}Zn_3(PO_4)_2 \cdot 4H_2O(s)$		372.7	-4102.0	-3628.9	23
$Zn_3(PO_4)_2 \cdot 2H_2O(s)$	-	243.0	-3516.3	-3143.5	23
$Zn_3(PO_4)_2 \cdot H_2O(s)$	-	184.3	-3211.7	-2890.9	23
$Zn_3(PO_4)_2(s)$		134.3	-2899.6	-2633.4	23
$Zn_2(OH)PO_4 \cdot 1.5H_2O(s)$				-1982.4 ± 3.1	24
$Zn_2(OH)PO_4(s)$		235.9	-1743.6	-1604.6 -1632.1 ± 4.0	This Work 24
$NaZnPO_4(s)$	150.3	169.0	-1622.4	-1510.6	1, This Work

lattice constants being caused by the smaller size of the Be(II) ion relative to the Zn(II) ion. On the other hand, the structural similarity between $NaZnPO_4$ and the $Na(Zn_{0.8}Fe_{0.2})PO_4$ compound reported by Kabalov et al[6] indicates that zinc(II) oxide decomposition in the presence of solubilized Fe(II) ions may lead to crystallization of an 'impure' sodium zinc phosphate precipitate that represents a solid solution of Zn(II) and Fe(II) ions - $Na(Zn_{1-x}Fe_x)PO_4$. The incorporation of Fe(II), however, may cause slight lattice distortions which lead to a monoclinic cell, i.e., 90 → 90.2 deg.

To more fully interpret the significance of formation of a sodium-less ZnO decomposition product in alkaline sodium phosphate solutions having Na/P ≥ 2.0, a comparison of equilibrium constants associated with the formation of some zinc phosphate minerals expected to exist in the $ZnO-P_2O_5-H_2O$ ternary oxide system is given in Table VIII. These estimates were derived from recent room temperature solubility studies for α-hopeite[26], tarbuttite[24], and spencerite[24]. Based on the Table VII compilation, ΔG° estimates (hence equilibrium constants) were obtained for potential ZnO decomposition reactions. The calculated threshold concentrations of $H_3PO_4(aq)$ required to initiate these reactions are compared in Table VIII. This comparison reveals that the tarbuttite formation reaction requires the lowest concentrations of $H_3PO_4(aq)$ in order to procede. Since the initial solutions for Tests 9 - 11 had room temperature log $[H_3PO_4(aq)]$ values that ranged between -14.4 and -15.5, and were higher than in the first eight runs, it is seen that temperature increases were sufficient to cause the $ZnO/Zn_2(OH)PO_4$ phase boundary to be crossed.

TABLE VIII

Estimated Reaction Thresholds for Zinc(II) Oxide
Decomposition in the $ZnO-P_2O_5-H_2O$ Ternary Oxide System

Decomposition Reaction	$\Delta G°$ kJ/mol	log $[H_3PO_4(aq)]$ mol/kg
$2ZnO(s)+H_3PO_4(aq)+1/2H_2O \rightleftarrows Zn_2(OH)PO_4 \cdot 1.5H_2O(s)$	-78.94	-13.831
$2ZnO(s)+H_3PO_4(aq) \rightleftarrows Zn_2(OH)PO_4(s)+H_2O$	-84.42	-14.791
$3ZnO(s)+2H_3PO_4(aq)+H_2O \rightleftarrows \alpha\text{-}Zn_3(PO_4)_2 \cdot 4H_2O(s)$	-142.89	-12.518
$3ZnO(s)+2H_3PO_4(aq) \rightleftarrows Zn_3(PO_4)_2 \cdot 2H_2O+H_2O$	-131.65	-11.533
$3ZnO(s)+2H_3PO_4(aq) \rightleftarrows Zn_3(PO_4)_2 \cdot H_2O+2H_2O$	-116.43	-10.200

An inconsistency exists with regard to the $ZnO/Zn_2(OH)PO_4$ phase boundary, since the present three high temperature points do not extrapolate linearly to the implied room temperature estimate[24] (see Figure 5). It is noted that the initial (i.e., room temperature) H_3PO_4(aq) concentration used in test 11 was greater than the implied H_3PO_4(aq) threshold concentration for Eqn. (3), based on the results of Magalhaes et al[24]. Therefore, the true ΔG° value for Eqn. (3) must be greater than -81.98 kJ/mol. Considering the reported uncertainty in ΔG_f° for tarbuttite formation ($\pm$4.0 kJ/mol per Table VII), and invoking a 2σ limit, allows an upper limit of ΔG° = -76.4 kJ/mol to be derived for Eqn. (3) using the results of Magalhaes et al[24]. This estimate differs by ~ 19 kJ/mol from one based on extrapolation of the Eqn. (3) equilibrium via Eqn. (14): ΔG° = -57.0 kJ/mol. The presently extrapolated thermochemical parameters for tarbuttite are considered tentative, pending completion of a ZnO phase stability study in sodium phosphate solutions having Na/P $\leq$ 2.

REFERENCES

1. S.E. Ziemniak, M.E. Jones and K.E.S. Combs, J. Solution Chem. 24, 1153 (1992)
2. E. Thilo and I. Schulz, Z. anorg. allg. Chemie 265, 14 (1951)
3. S.E. Ziemniak and E.P. Opalka, Chem. Mater. 5, 690 (1993)
4. JCPDS Powder Diffraction File, Sets 1-39, International Centre for Diffraction Data, Swarthmore, PA (1989)
5. A.-W. Kolsi, A. Erb and W. Freundlich, C.R. Acad. Sci. Paris, Ser. C 282, 575 (1976)
6. Yu.K.Kabalov, M. A. Simonov, O. K. Mel'nikov and N. V. Belov, Soviet Phys. - Dokl. 17, 835 (1973)
7. D. Louer and M. Louer, J. Appl. Cryst. 5, 271 (1972)

8. A. R. Milnes and R. J. Hill, Neues Jahrb. Mineral., Monatsh. (1), 25 (1977)

9. Yu. K. Kabalov, M. A. Simonov, O. V. Yakubovich and N. V. Belov, Soviet Phys. - Dokl. 18, 627 (1974)

10. Yu. K. Kabalov, M. A. Simonov and N. V. Belov, Soviet Phys. - Dokl. 17, 77 (1972)

11. W.L. Marshall and E.V. Jones, J. Phys. Chem. 70, 4028 (1966)

12. F.H. Sweeton, R.E. Mesmer and C.F. Baes, J. Solution Chem. 3, 191 (1974)

13. R. E. Mesmer and C. F. Baes, J. Solution Chem. 3, 307 (1974)

14. N. C. Treloar, Central Electricity Research Laboratory Report RD/L/N 270/73 (1973). (See WAPD-TM-1302, March 1979)

15. I. L. Khodakovskii, B. N. Ryzhenko and G. B. Naumaov, Geochem. Int. 5, 1200 (1968)

16. R.M. Izatt, J.J. Christensen, J.L. Oscarson, and S.E. Gillespie, J. Solution Chem. 17, 841 (1988)

17. C. M. Criss and J. W. Cobble, J. Amer. Chem. Soc. 86, 5390 (1964)

18. M. H. Abraham and Y. Marcus, J. Chem. Soc., Faraday Trans. 1, 82, 3255 (1986)

19. D. D. Wagman, W. H. Evans, V. B. Parker, R.H. Schumm, I. Halow, S. M. Bailey, K. L. Churney, and R. L. Nuttall, J. Phys. Chem. Ref. Data, 11, Suppl. 2 (1982)

20. I. L. Khodakovskii and A. E. Elkin, Geokhimiya 10, 1490 (1975)

21. O. Kubaschewski and C. B. Alcock, Metallurgical Thermochemistry, Pergamon Press, Oxford (1983)

22. J. W. Larson, K. G. Zeeb and L. G. Hepler, Can. J. Chem. 60, 2141 (1982)

23. P. Vieillard and Y. Tardy, in Phosphate Minerals, eds, J. O. Nriagu and P. B. Moore (Springer-Verlag, Berlin, 1984), Ch. 4

24. M. C. F. Magalhaes, J. P. deJesus and P. A. Williams, Mineral. Mag. 50, 33 (1986)

25. N. I. Golovastikov, Soviet Phys. - Crystallogr. 6, 733 (1962)

26. J. O. Nriagu, Geochim. Cosmochim. Acta 37, 2357 (1973)

DATE
FILMED
1/11/94
END